frontiers
in Ecology and Evolution

Soil Moisture but Not Warming Dominates Nitrous Oxide Emissions During Freeze–Thaw Cycles in a Qinghai–Tibetan Plateau Alpine Meadow With Discontinuous Permafrost

Zhe Chen[1,2,3,4], Shidong Ge[5], Zhenhua Zhang[3], Yangong Du[3], Buqing Yao[3], Huichun Xie[1,2,3,4], Pan Liu[1], Yufang Zhang[1], Wenying Wang[1,2,3,4]* and Huakun Zhou[3]*

[1] College of Life Sciences, Qinghai Normal University, Xining, China, [2] Academy of Plateau Science and Sustainability, Xining, China, [3] Qinghai Provincial Key Laboratory of Restoration Ecology for Cold Regions, Northwest Institute of Plateau Biology, Chinese Academy of Sciences, Xining, China, [4] Qinghai Provincial Key Laboratory of Medicinal Animals and Plants Resources in Qinghai-Tibet Plateau, Qinghai Normal University, Xining, China, [5] College of Landscape Architecture and Art, Henan Agricultural University, Zhengzhou, China

OPEN ACCESS

Large quantities of organic matter are stored in frozen soils (permafrost) within the Qinghai–Tibetan Plateau (QTP). The most of QTP regions in particular have experienced significant warming and wetting over the past 50 years, and this warming trend is projected to intensify in the future. Such climate change will likely alter the soil freeze–thaw pattern in permafrost active layer and toward significant greenhouse gas nitrous oxide (N_2O) release. However, the interaction effect of warming and altered soil moisture on N_2O emission during freezing and thawing is unclear. Here, we used simulation experiments to test how changes in N_2O flux relate to different thawing temperatures (T^5–5°C, T^{10}–10°C, and T^{20}–20°C) and soil volumetric water contents (VWCs, W^{15}–15%, W^{30}–30%, and W^{45}–45%) under 165 F–T cycles in topsoil (0–20 cm) of an alpine meadow with discontinuous permafrost in the QTP. First, in contrast to the prevailing view, soil moisture but not thawing temperature dominated the large N_2O pulses during F–T events. The maximum emissions, 1,123.16–5,849.54 μg m^{-2} h^{-1}, appeared in the range of soil VWC from 17% to 38%. However, the mean N_2O fluxes had no significant difference between different thawing temperatures when soil was dry or waterlogged. Second, in medium soil moisture, low thawing temperature is more able to promote soil N_2O emission than high temperature. For example, the peak value (5,849.54 μg m^{-2} h^{-1}) and cumulative emissions (366.6 mg m^{-2}) of $W^{30}T^5$ treatment were five times and two to four times higher than $W^{30}T^{10}$ and $W^{30}T^{20}$, respectively. Third, during long-term freeze–thaw cycles, the patterns of cumulative N_2O emissions were related to soil moisture. treatments; on the contrary, the cumulative emissions of W^{45} treatments slowly increased until more than 80 cycles. Finally, long-term freeze–thaw cycles could improve nitrogen availability, prolong N_2O release time, and increase N_2O cumulative emission in permafrost active layer. Particularly, the high emission was

concentrated in the first 27 and 48 cycles in W^{15} and W^{30}, respectively. Overall, our study highlighted that large emissions of N_2O in F–T events tend to occur in medium moisture soil at lower thawing temperature; the increased number of F–T cycles may enhance N_2O emission and nitrogen mineralization in permafrost active layer.

Keywords: global climate change, nitrous oxide, permafrost active layer, freeze–thaw, nitrogen transformation

INTRODUCTION

The global permafrost and seasonally frozen ground cover about 70% of all terrestrial ecosystems (Lawrence et al., 2012). In cold regions, soil freeze–thaw (F–T) events are a key natural process driving soil aggregate fragmentation (Chai et al., 2014), organic matter activization (Chen L. et al., 2016), root death (Kreyling et al., 2012), changes in microbial community structure and function (Yang et al., 2018; Mao et al., 2019), and available nitrogen (N) transformation (Jiang et al., 2020; Mao et al., 2020). These process changes in a warmer world are further intensifying nitrous oxide (N_2O) release from permafrost and seasonally frozen zones (Henry, 2008; Brooks et al., 2011; Risk et al., 2013; Chen et al., 2018; Lv et al., 2020).

Global warming is profoundly altering soil F–T patterns by increasing the thickness of the permafrost active layer, reducing days of the frozen period, and increasing days of the thawing period (Henry, 2008; Elberling et al., 2013; Schuur et al., 2015; Lin et al., 2017). Moreover, the decreasing precipitation in winter (Gaëlle et al., 2011) would cause the topsoil to undergo more frequent F–T cycles because of a lack of insulation from snow cover (Wipf et al., 2015) and, consequently, accelerate soil organic matter decomposition (Bracho et al., 2016). All these changes would provide favorable microenvironments and sufficient feedstock for excessive use of N by soil microbial nitrification–denitrification (Teepe et al., 2001). However, the magnitude of F–T effects on the key process of N transformation, particularly N_2O emissions, in high latitude and/or high-altitude regions remains highly uncertain.

N_2O is a product of nitrification and denitrification, and a potent greenhouse gas with about 265 times more warming potential than CO_2 over a 100-year period (IPCC, 2013). During recent F–T events, significant soil N_2O emissions have been reported in different types of cold ecosystems (Wu et al., 2020; Li et al., 2021). We synthesized some existing studies and found that the amount of N_2O released ranged from 0.7 to 27.2 kg N ha^{-1} during the nongrowing season (October–April), accounting for 10–80% of their total annual ecosystem soil emissions (Chen et al., 2018). Thus, in cold regions, the large N_2O emissions during F–T cycles are not only a crucial part of the soil N pool loss but also a non-negligible global greenhouse gas source, with CO_2 release from widespread permafrost thawing (Wang et al., 2014; Schuur et al., 2015; Song et al., 2015; Lv et al., 2020).

Unfortunately, despite being an indicator of global climate change, N_2O emissions during the F–T period from alpine grasslands in the Qinghai–Tibetan Plateau (QTP) are rarely reported. Moreover, the permafrost soil environment in the QTP has become more complicated under climate change. The overall warming rate of the QTP ranges from 0.16 to 0.67°C decade^{-1}, and the temperature increase in winter (0.45°C 10 a^{-1}) is nearly twice that in summer (Qin, 2014). An *in situ* warming experiment showed that the thickness of the seasonally frozen ground would decrease by 14.8% when the temperature of surface soil in the alpine meadow increases 2.03–2.3°C, the frozen period would decrease by 44–83 days, and the number of day–night F–T cycle days in the topsoil during spring would increase by 37–44 days (Lin et al., 2017). The annual precipitation is also increasing in most areas of the QTP, while some subregions are becoming drier (Kuang and Jiao, 2016). On account of the large specific heat capacity of water, the slight fluctuation of soil moisture will significantly change the process of soil heat exchange during the F–T process (Fang et al., 2016). Thus, it is worth studying the interaction effect of warming and altered soil moisture on N_2O emission during freezing and thawing.

Most single-factor studies suggest that large soil N_2O emissions are significantly affected by thawing temperature (Yao et al., 2010), and the emissions occur over a few F–T cycles (Teepe et al., 2001; Bollmann and Conrad, 2004; Wu et al., 2019). However, our previous *in situ* study showed that soil temperature had no significant correlation with the N_2O fluxes during spring thawing because the snow-cover thawing increased soil water content and led to the surface soil remaining at about 0°C for a long time (Chen et al., 2018). The short pulses of N_2O emission resulted from the combined impact of high soil moisture and flush available nitrogen (Yao et al., 2010; Lu et al., 2015a,b; Jiang et al., 2020; Wu et al., 2020). In view of the synchronous change in temperature and precipitation on the QTP, the first question we would like to explore was how N_2O emissions respond to different moisture and thawing temperature gradations during the F–T process.

Our second aim was to determine whether soil N_2O emissions in the QTP permafrost region are closely related to the number of F–T cycles. It is still difficult to accurately capture N_2O emissions during soil freezing or thawing in the field without real-time online monitoring instruments. These conditions are unfavorable for assessing greenhouse gas emissions during nongrowing seasons in high latitudes or elevation regions. Thus, we aimed to create a model of N_2O flux pattern under the coupled conditions of varying temperature and moisture gradients. Based on the above objectives, this study used long-term F–T cycle laboratory experiments to test QTP alpine meadow soil N_2O dynamics and determine the relationship between N_2O flux and soil F–T environmental factors. Ultimately, the results of this study would provide guidance for further discussion of the ecological effects of F–T on the soil N cycle in the QTP permafrost under climate change.

MATERIALS AND METHODS

Site Description

Soil samples were collected from Daban Mountain (37°20′16.93″N, 101°23′47.21″E, 3,705 m a.s.l.), located in the eastern part of the Qilian Mountains in Qinghai Province. The area has a typical plateau continental climate, with a long cold winter and short warm summer. The annual average temperature was −1.6°C, with the maximum monthly mean temperature in July (10.1°C) and the minimum monthly mean temperature in January (−15.0°C). The historical extreme maximum and minimum temperatures were 26.8 and −37.1°C, respectively. The number of days with a daily minimum temperature below 0°C during the year was as high as 280 days. The annual precipitation was 560 mm, on average, of which 85% was concentrated in May–September. The regional annual mean evaporation was 1,238.0 mm (Li et al., 2004; Dai et al., 2019). The dominant species is *Kobresia pygmaea*, and it is associated with *Saussurea*, *Potentilla*, *Leontopodium*, *Gentian*, *Saxifraga*, *Poa*, *Oxytropis*, and *Polygonum*. The average height of vegetation was < 10 cm, and the aboveground dry biomass averages 210 g m^{-2}.

Soil samples were collected in a transition zone of seasonal permafrost and spot (island) permafrost, and the soil was classified as Inceptisol or Cambisol. The topsoil (0–10 cm) organic matter, bulk density, pH, and soil volume water content in *K. humilis* meadow are 138.52 ± 13.82 g kg^{-1}, 0.75 ± 0.05 g cm^{-3}, 7.50 ± 0.22, and 32.7% ± 5.17%, respectively (Wang et al., 2011). The site froze from late October to mid-November. A stable thin permafrost layer began to form in late November, and the thickness of the permafrost continued to increase and reached the maximum freezing depth of 0.5–1 m in mid-February of the following year. The soil began to enter the thawing period in early March, and the thaw depth continued to increase until thawing was complete by late April (Lin et al., 2017; Dai et al., 2019).

Experimental Design

We used soil VWC to express the level of soil moisture. Three VWC values (W^{15}–15%, W^{30}–30%, and W^{45}–45%) and three thawing temperature (T^5–5°C, T^{10}–10°C, and T^{20}–20°C) levels were applied in a randomized complete block design, for nine total treatments and three replications for each treatment. The topsoil of the study site usually begins to thaw from early-March to mid-April (Lin et al., 2017; Dai et al., 2019), and during this time, the day air temperatures fluctuate between 0°C and 13°C. Therefore, the 5°C of thawing temperature in our study was used as the control temperature. The 10°C of thawing temperature could represent the century-scale warming trend (2–7°C) of the QTP (Qin, 2014). The 20°C means extreme high temperature. According to our pre-experiment, the maximum volumetric water content was about 45%, and field study showed that the soil moisture in the growing season (July–August) were maintained at about 25%–35% VWC. Thus, we take the 30% VWC as the medium soil water. The difference in moisture gradient was controlled by 15% VWC. The existing precipitation control test also set treatments with natural and 50% reduction or increase in rainfall in an alpine grassland on the northeastern Tibetan Plateau (Xu et al., 2017).

In early July 2019, we set three 1-m × 1-m plots in the experiment site, then cut off the aboveground biomass, collected a sufficient amount of top soil (0–20 cm) with a drill (diameter 10 cm), and brought soil back to the laboratory the same day. After removing dead grass litter, plant roots, and gravel (grain diameter > 2 mm), 500 g of soil was weighed and transferred to a 1-L glass jar; then, the bottle was shaken to ensure that the soil contacted the bottle. The height of the soil in the bottle was 8–10 cm, and the soil surface was 11–13 cm away from the bottle plug. The plastic plugs of each bottle had three holes, two of which were connected to a rubber tube and a three-way valve. One of the three-way valves was linked with sampling needle tubing (10 ml), and the other valve was connected with the needle tubing (100 ml) to balance the bottle pressure. The third hole was used to hold the probe thermometer for recording the air temperature in each bottle. The interfaces of the holes were treated with latex to ensure airtightness. A time-domain reflectometer was used to measure soil moisture, which was adjusted in every treatment to the required VWC by adding ultrapure water. Each bottle was measured every 5 days during the whole test, and according to the change in mass, ultrapure water was added to keep the soil moisture stable.

Because the daily maximum temperature in the study area was nearly 15°C when we collected the samples, in order to make the test soil microbial community as consistent as possible with the early cold season, all samples were successively incubated at 15°C, 10°C, and 5°C for 1 week. After the cold acclimation, samples were put in three different incubators, and day and night F–T treatment was initiated. The freezing temperature was set as −20°C from 20:00 to 8:00 the next day, and thawing temperatures were set as 5°C, 10°C, and 20°C from 08:00 to 20:00. On the day of sampling, the freezing time were reduced by 90 min (21:30 to 08:00 the next day). The F–T cycles lasted about 165 days.

N$_2$O Flux Measurements

Gas collection and measurement were similar to the static chamber-gas chromatography method. Gasses were sampled once a day during the first 7 days, then once every 3 days from the 8th to 22nd day, once every 5 days from the 23rd to 48th day, and once every 7 days from the 49th to 165th days. The gas collection began at 20:00, and after the bottle was closed, a 10-ml gas sample was taken from the bottle with a plastic syringe at 0, 30, 60, and 90 min. Every time before the gas sample was drawn, the syringe piston was quickly pushed and pulled twice to stir and mix the air in the bottle. The three-way valves of the air intake channel were kept closed between the sampling intervals. We recorded the air temperature inside and outside of the bottle at every sampling, which were used to correct the N$_2$O flux. The soil surface temperatures of each treatment were measured with an infrared detector.

The N$_2$O concentration of the gas sample was analyzed within 24 h using gas chromatography (Agilent 7890A, Agilent Technologies, Sta Clara, CA, United States). The N$_2$O flux was

calculated according to the following equation:

$$F = \frac{dc}{dt} \cdot \frac{M}{V_0} \cdot \frac{P}{P_0} \cdot \frac{T_0}{T} \cdot H$$

where F (μg m^{-2} h^{-1}) is the N_2O flux; dc/dt is the slope of the linear regression for the N_2O concentration gradient as a function of time; M (g mol^{-1}) is the molecular mass of N_2O; P (Pa) is the atmospheric pressure; T (K) is the absolute temperature during sampling; V_0 (L), T_0 (K), and P_0 (Pa) are the gas mole volume, absolute air temperature, and atmospheric pressure under standard condition, respectively; and H (m) is the height of the soil surface to the bottle plug (Chen et al., 2018).

Data Analysis

All data were assessed for normality of variance before analysis. First, the effects of VWC, temperature, number of F–T cycles, and their interactions on mean N_2O flux were investigated using general linear-model multivariate analysis. In the model, the significant differences in the mean N_2O fluxes between the treatments based on a least significant difference (LSD) test (IBM SPSS Statistics 20.0, SPSS Inc., Chicago, IL, United States). Second, a quarter of the measured N_2O flux was used to represent the daily mean emission rate, and the cumulative emissions were estimated using a linear interpolation method. Finally, linear, polynomial, exponential, and peak functions were used for fitting N_2O flux and soil moisture and temperature in OriginPro 2020b (OriginLab Corp., Northampton, MA, United States). The models with the highest fitting degree were selected to represent the regression relationship between N_2O flux and other environmental factors. All significant differences were at 0.05 (α).

RESULTS

N_2O Flux Pattern in Freeze–Thaw Cycles

The N_2O emissions of W^{30} treatment were higher than W^{15} and W^{45}, and its patterns were similar even at different thawing temperatures. **Figures 1A-1,B-1,C-1** shows that the emission periods of W^{30} treatment were concentrated in the first 48 cycles, and the peak value occurred at the 13th F–T cycle. The peaks of $W^{30}T^5$, $W^{30}T^{10}$, and $W^{30}T^{20}$ were, respectively, 5,849.54, 1,123.16, and 1,253.83 μg m^{-2} h^{-1}, which were 1,466.05, 335.27, and 327.37 times higher than the initial values. However, the major emissions of the W^1 group occurred from 1 to 27 days, the emission peak (190.78–223.27 μg m^{-2} h^{-1}) occurred after the third or fourth F–T cycle and was only 1.55–1.85 times that at the beginning of the F–T cycles. Instead of increasing, the fluxes of W^{45} treatments dropped sharply after the first cycle and were maintained at between −2.95 and 13.69 μg m^{-2} h^{-1} during all F–T cycles.

Variance analysis also indicated that at the same thawing temperature, the average fluxes of W^{30} treatment were significantly higher than those of W^{15}, and the W^{45} treatment had the lowest fluxes (**Figures 1A-2,B-2,C-2**). At the same moisture, the average fluxes were not significantly different between different thawing temperatures in the W^{15} and W^{45}

groups, but the mean flux of $W^{30}T^5$ (747.02 μg m^{-2} h^{-1}) was significantly higher than that of $W^{30}T^{20}$ (363.99 μg m^{-2} h^{-1}), and $W^{30}T^{10}$ (220.41 μg m^{-2} h^{-1}) was the lowest.

The Pattern of N_2O Cumulative Emissions During Long-Term Freeze–Thaw Cycles

The three soil moisture levels showed three cumulative emission patterns. The total cumulative emissions of the W^{30} group were the highest (102.04–366.6 mg m^{-2}), followed by the W^{15} group (24.96–34.18 mg m^{-2}) and the W^{45} group (0.81–2.96 mg·m^{-2}). In the W^{15} group, the N_2O cumulative emissions continued increasing over all F–T cycles (average accumulation rate, 0.19 mg m^{-2} day^{-1}) (**Figures 2A–C**). The accumulations of the W^{30} group were mainly reflected at the beginning of F–T cycles (average accumulation rate, 8.3 mg m^{-2} day^{-1}) and increased minimally after 60 cycles (**Figures 2D–F**). However, N_2O fluxes of the W^{45} group were low in early F–T cycles, only increasing after 80 cycles, primarily in W^{45} (**Figures 2G–I**).

Dynamics of the Ammonium and Nitrate Contents

During the early freeze–thaw cycle, ammonium increased significantly in all treatments, and the peak value range from 57.42 to 188.80 mg kg^{-1} (**Figures 3A-1,B-1,C-1**). The increase in soil ammonium contents coincided with N_2O large emission in W^{15} and W^{30}. Although the peak ammonium contents in the water-saturated soil were higher than other treatments at the early freeze–thaw stage, there was no significant N_2O emissions. The nitrate content increased sharply in $W^{30}T^5$ during early freeze–thaw cycle, and the peak value of nitrate content was nearly 24.11 mg kg^{-1} (**Figure 3A-2**). Meanwhile, only low thawing temperature (T^5) improved nitrate accumulation after long freeze–thaw cycles (**Figures 3A-2,B-2,C-2**).

Relationship Between N_2O Flux and Freeze–Thaw Environmental Factors

The results showed that soil moisture, thawing temperature, and the number of F–T cycles all had significant impacts on N_2O flux, and their interactions were significant ($P < 0.01$) (**Table 1**). **Figure 4** shows that the flux response to soil moisture during F-T cycles conformed to the Gauss Amp function at the three different thawing temperatures ($P < 0.01$). In the range of VWC 15–45%, N_2O flux variations were "unimodal." The peak emission values of T^5, T^{10}, and T^{20} treatments were at VWC 27%, 25%, and 30%, respectively, and the 95% confidence intervals were, respectively, 22–32%, 17–32%, and 22–38% (**Figure 4**). These results highlighted that the medium level of soil water was essential in controlling large N_2O emissions during F–T cycles.

There were no correlations between the N_2O flux and thawing temperature in the W^{15} and W^{45} groups (**Figures 5A,C**). The response of flux to temperature showed a polynomial relationship ($P = 0.02$) in the W^{30} treatment, and it increased with the temperature increase in the range of 0°C to 5°C, then decreased in the range of 5–10°C and increased again from 10°C to 20°C (**Figure 5B**). This suggested that the N_2O flux was mostly
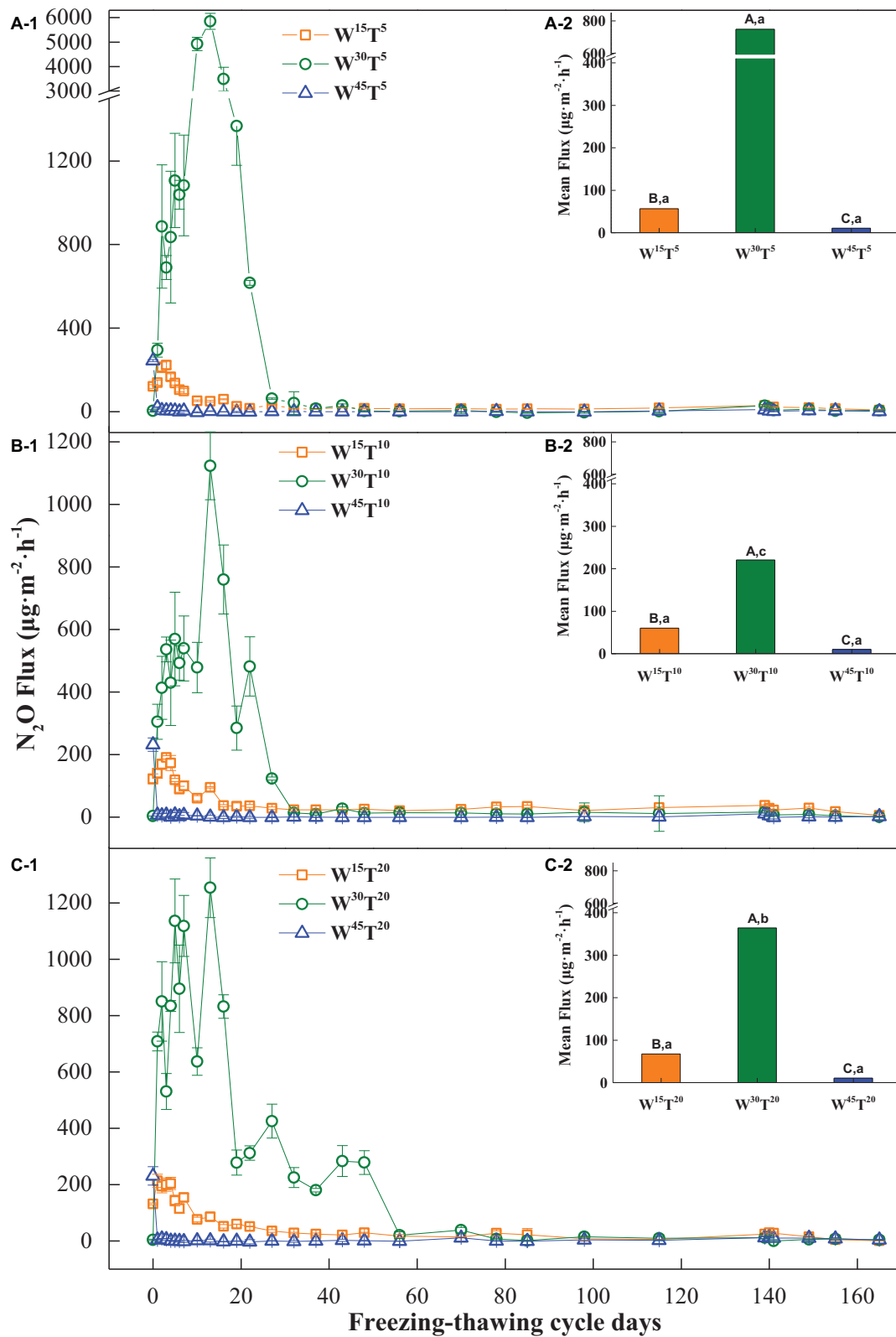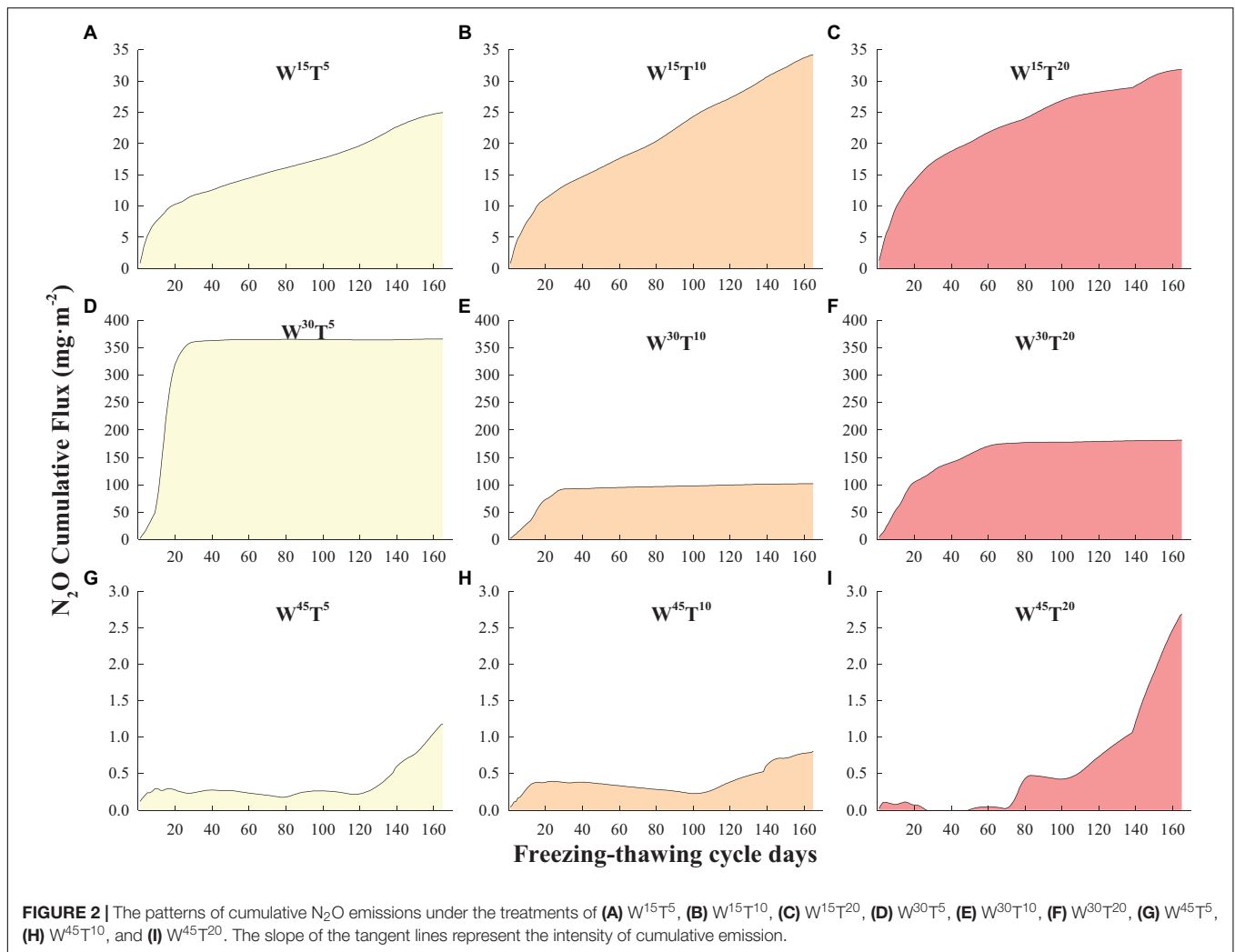
FIGURE 1 | (A-1,**B-1**,**C-1)** Dynamics and **(A-2**,**B-2**,**C-2)** average flux of N_2O during freeze–thaw cycles. Capital letters above each bar indicate significant differences between different soil moistures with the same thawing temperature, and the lowercase letters indicate significant differences between different thawing temperatures with the same soil moisture.

FIGURE 2 | The patterns of cumulative N$_2$O emissions under the treatments of **(A)** W^{15}T^5, **(B)** W^{15}T^{10}, **(C)** W^{15}T^{20}, **(D)** W^{30}T^5, **(E)** W^{30}T^{10}, **(F)** W^{30}T^{20}, **(G)** W^{45}T^5, **(H)** W^{45}T^{10}, and **(I)** W^{45}T^{20}. The slope of the tangent lines represent the intensity of cumulative emission.

influenced by a medium moisture level in soil, and the large N$_2$O emissions during F–T cycles had complicated nonlinear relationships with the thawing temperature.

Model of N$_2$O Flux During Short-Term Freeze–Thaw Cycles

Based on the relationship between soil N$_2$O dynamics and soil water and thawing temperature in the first 48 F–T cycles (large emission period), we drew the diagram of N$_2$O flux model (**Figure 6**). We speculated that the medium moisture controlled the large production and release of N$_2$O over F–T cycles. Because of appropriate soil, porosity tends to result in abundant aerobic and anaerobic microenvironments. These microzones were especially common at low thawing temperatures when the ice crystals in deep soil do not melt completely and coexist with soil air and free water, simultaneously promoting nitrification and denitrification. However, under dry conditions, the vast aerobic environment was beneficial to nitrification, and some N$_2$O was released as the nitrification by-product. For the high soil water content, N$_2$O production was dominated by denitrification,

and the large intermediate products of N$_2$O were completely converted to N$_2$ under an anaerobic environment. Moreover, under high moisture, the large interstices of deep soil were filled with water or ice, and the upper layer was covered with water. These physical barriers would block N$_2$O emissions and greatly reduce N$_2$O flux when frozen soil was thawing. The effect of thawing temperatures on the redox conditions of dry and waterlogged soil was limited, so the response of soil N$_2$O flux to thawing temperature tended to be consistent in these two states.

DISCUSSION

The Effects of Abiotic and Nitrogen Transformation on N$_2$O Flux During the Freeze–Thaw Cycles

We found that no matter how the thawing temperature changed, the N$_2$O fluxes had significant peak functions with soil VWC, and the 95% confidence intervals ranged from 17 to 38% (VWC). These findings show that the relationship between soil moisture and N$_2$O flux during F–T cycles was not linear, and a medium
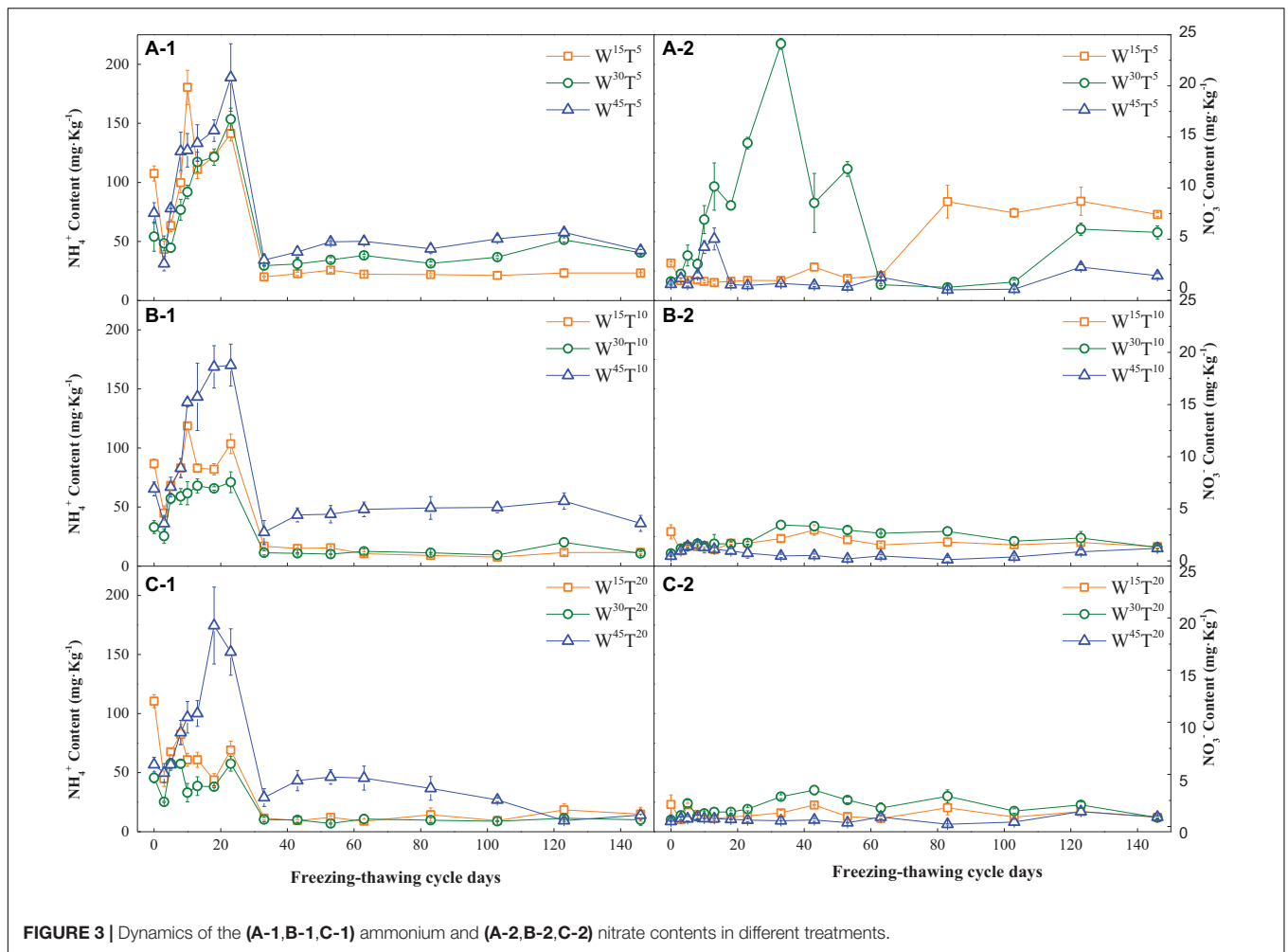
FIGURE 3 | Dynamics of the **(A-1**,**B-1**,**C-1)** ammonium and **(A-2**,**B-2**,**C-2)** nitrate contents in different treatments.

level of moisture is more likely to promote N_2O emissions. In contrast, when the soil was dry or waterlogged, N_2O emissions were sharply reduced during F–T. Our previous *in situ* test of seasonal frozen arable soils in northeast China also indicated that soil moisture explained 32% of the N_2O flux variation, and high soil moisture (30–55%) triggered the N_2O burst during the spring thaw (Chen et al., 2018). Quick warming of the bare soil

after snow melt resulted in rapidly decreased water content that returned to normal along with N_2O flux (Chen et al., 2018). However, in our earlier research, the soil moisture (55%) at

TABLE 1 | Test of soil moisture (W), thawing temperature (T), and freeze–thaw cycles (FTCs) effects on N_2O flux in the general linear model.

Factor	*F*-value	P
W	2,553.147	< 0.01
T	402.0377	< 0.01
FTCs	192.810	< 0.01
W × T	404.293	< 0.01
W × FTCs	178.947	< 0.01
T × FTCs	80.402	< 0.01
W × T × FTCs	81.691	< 0.01

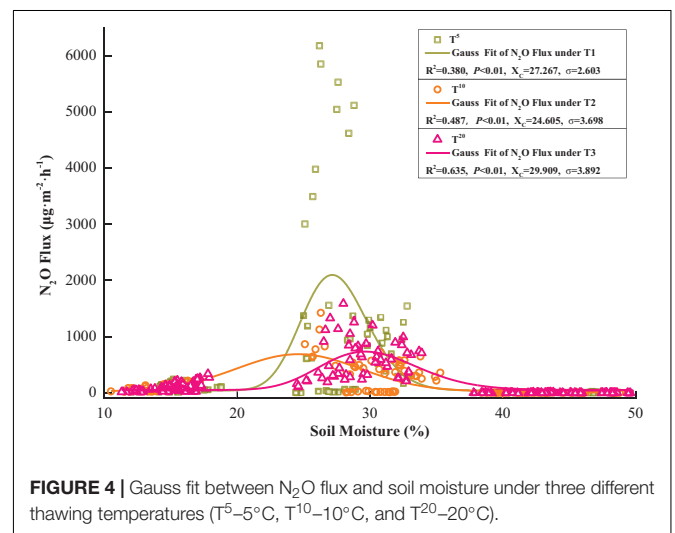*P < 0.01 means that the factor has a significant main effect or interaction effect on flux.*

FIGURE 4 | Gauss fit between N_2O flux and soil moisture under three different thawing temperatures (T^5–5°C, T^{10}–10°C, and T^{20}–20°C).
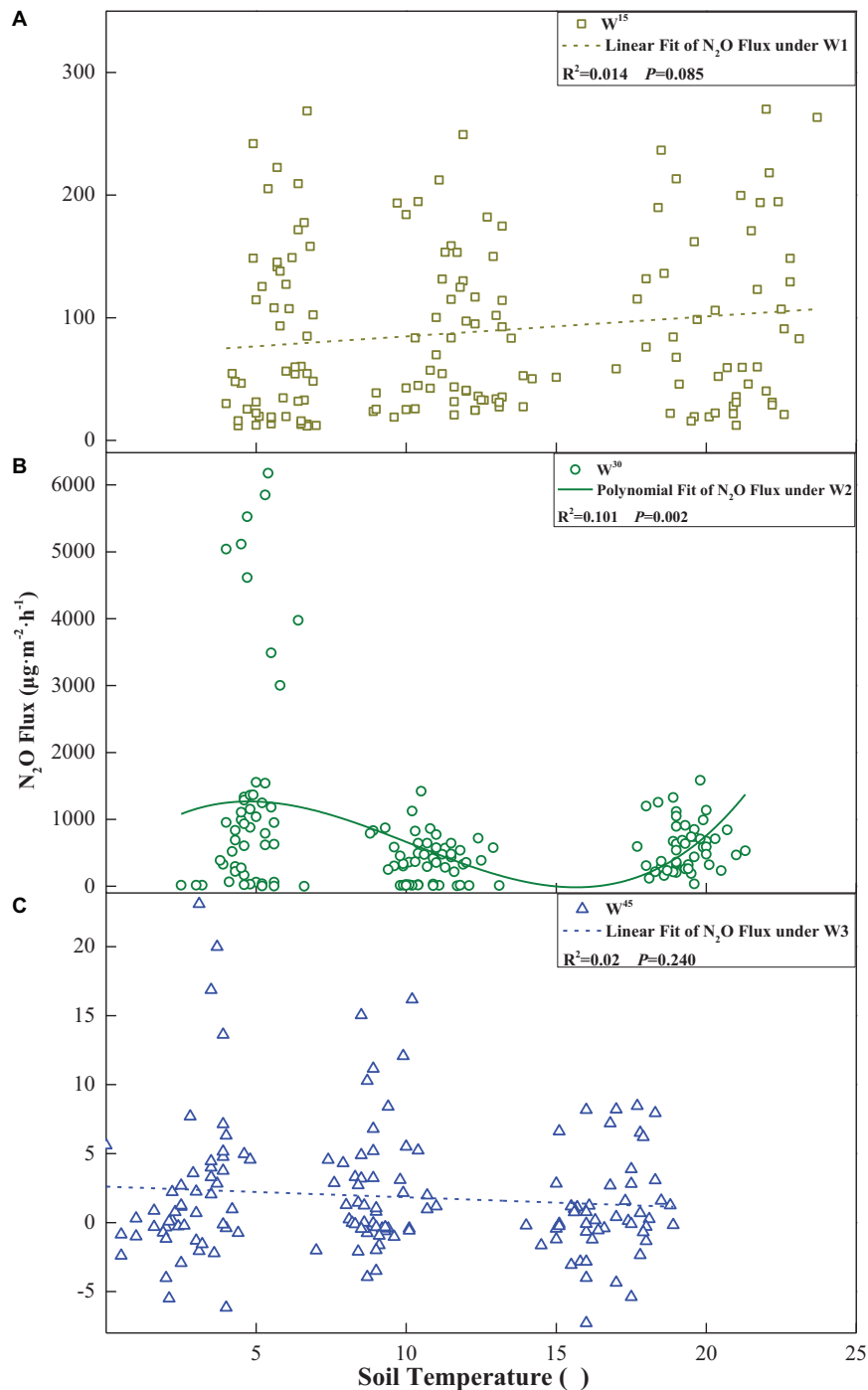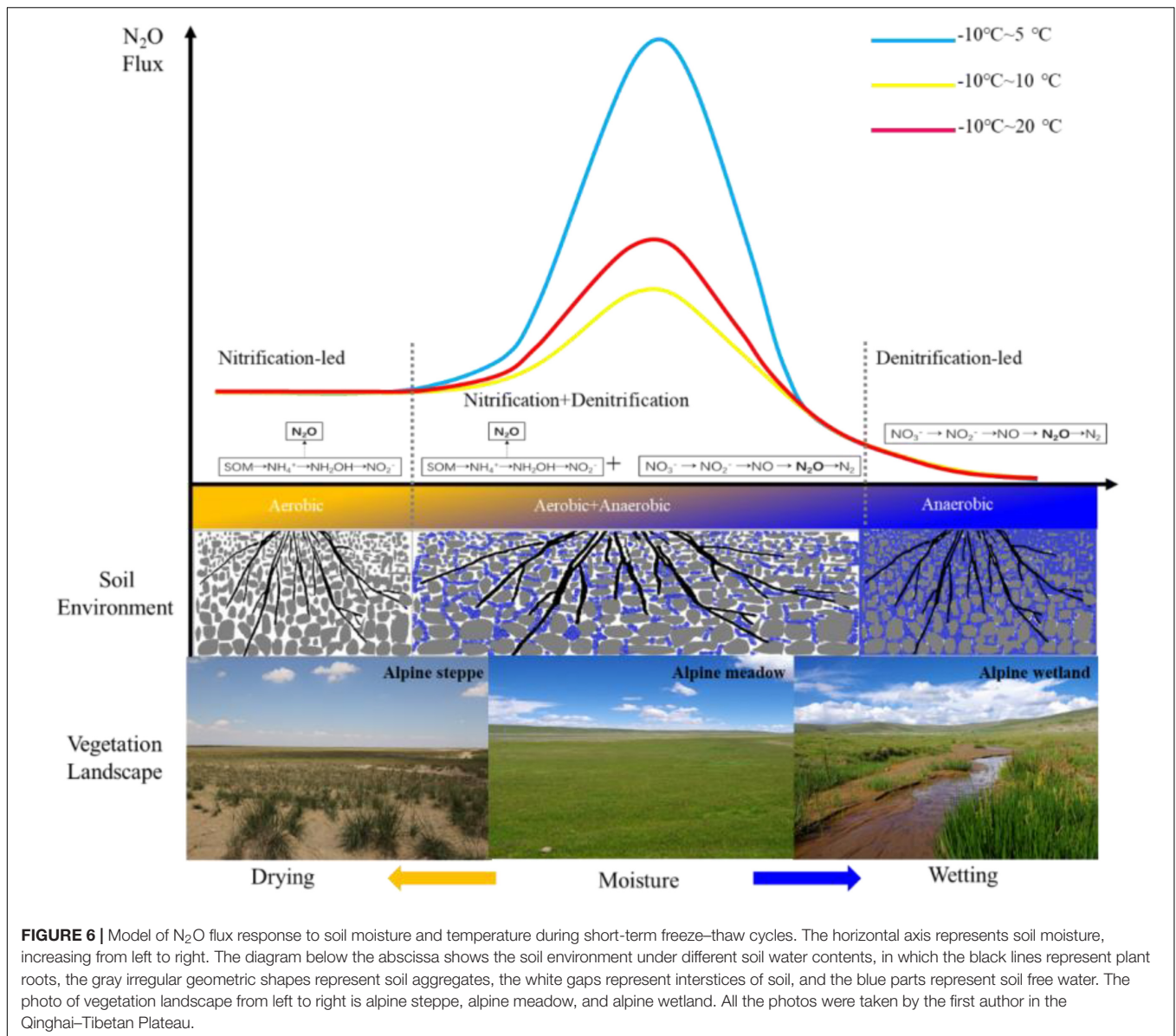
FIGURE 5 | The fitting results between N$_2$O flux and thawing temperature under soil volumetric water content of **(A)** 15%, **(B)** 30%, and **(C)** 45%. Solid lines represent significant ($P < 0.05$) fitted curves, while the dotted line are not significant ($P > 0.05$).

maximum emissions was higher than in this study (17%–38%), which may be related to the high water-holding capacity of arable black soil (mollisols) (Chen et al., 2018).

Teepe et al. (2004) explained that N$_2$O emissions during thawing decreased in the order 64% > 55% > 42% [water-filled pore space (WFPS)], but the flux at 76% WFPS was less than
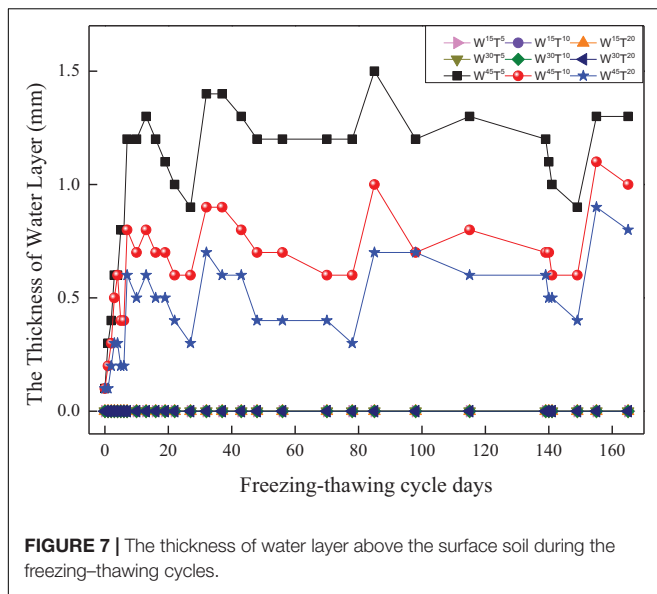
that at 55% WFPS. If our soil moisture were converted into WFPS, the peak values corresponding to the regression curve were 61% (T^5), 55% (T^{10}), and 66% (T^{20}). This means that the flux was positively correlated with the soil moisture when WFPS was lower than 55%, while it was negatively correlated with moisture when WFPS was higher than 66%. Thus, we assumed

FIGURE 6 | Model of N_2O flux response to soil moisture and temperature during short-term freeze–thaw cycles. The horizontal axis represents soil moisture, increasing from left to right. The diagram below the abscissa shows the soil environment under different soil water contents, in which the black lines represent plant roots, the gray irregular geometric shapes represent soil aggregates, the white gaps represent interstices of soil, and the blue parts represent soil free water. The photo of vegetation landscape from left to right is alpine steppe, alpine meadow, and alpine wetland. All the photos were taken by the first author in the Qinghai–Tibetan Plateau.

that the soil moisture had a threshold value to determine the large N_2O release during F–T. Other laboratory experiments also support our inference. For instance, Lu et al. (2015b,a) studied meadow-steppe grassland soil and found that N_2O emissions in F–T processes are 30 µg kg^{-1} h^{-1} when soil moisture was about 8% VWC; however, the flux plunged to 8.4 µg kg^{-1} h^{-1} in waterlogged soil. If soil water is a crucial factor that controls N_2O emissions during F–T, it is easy to understand why the current results of global N_2O variation are so large (0.7–27.2 kg N ha^{-1}) (Chen Z. et al., 2016). If more informed studies of *in situ* data of N_2O fluxes and soil moisture in the F–T period were integrated by meta-analysis, more meaningful and accurate conclusions may be obtained.

We suspected that the effects of soil moisture on N_2O emissions during F–T cycles were largely related to nitrification and denitrification, both of which generate N_2O and are

regulated by soil O_2 partial pressure. Studies show that, in dry soil, the N_2O emissions of nitrification increase as soil water content increases, and the release reaches a maximum when soil moisture is in the range of 45–55% maximum water holding capacity (WHC) (Bollmann and Conrad, 2004). N_2O emissions of denitrification in moist soils increase as soil water content increases, and maximum N_2O emissions were observed at 65–80% WHC (Bollmann and Conrad, 2004). Other studies found that denitrification is the major contributor of N_2O emissions under F–T environments, accounting for 80–90% of total N_2O emissions (Ludwig et al., 2004; Öquist et al., 2004; Yanai et al., 2007). Soil moisture in these studies was mostly maintained at 60% WFPS, similar to our W^2 group. In waterlogged soil, the N_2O fluxes maintained at a low level might be caused by an increased ratio of N_2/N_2O in the anaerobic environment (Teepe et al., 2004). Note that more N_2O is reduced to N_2 under high soil

FIGURE 7 | The thickness of water layer above the surface soil during the freezing–thawing cycles.

moisture. We also observed that the water level of the soil surface in W^{45} increased about 0.5–1.0 mm compared with the initial value (**Figure 7**). Previous studies have indicated that unfrozen soil water would be transferred from deep soil to upper layers during freezing (Dai et al., 2019). Thus, the increased water layer enhances the physical barrier and impedes soil N_2O outflow. It is inferred that when the soil water was below the threshold value, the positive correlation between N_2O flux and moisture was due to the accumulation of N_2O, as the by-product of nitrification and the product of nitrate are reduced by denitrifying bacteria (Ji et al., 2015). However, complete denitrification accelerates N_2O consumption, and aqueous barriers alleviate N_2O emissions when the moisture is high.

The soil N_2O emissions with moderate moisture under low thawing temperature (T^5) were much higher than in normal (T^{10}) and high temperature (T^{20}) treatments. Surprisingly, the peak flux of $W^{30}T^5$ was as high as 5,849.54 $\mu g \cdot m^{-2} \cdot h^{-1}$, which was the highest compared to all previous studies. Teepe et al. (2001) confirmed that frequent F–T cycles create abundant aerobic, anaerobic, or intermediate microzones, which are favorable for nitrification and denitrification. Consistent with Teepe et al. (2001), we observed that the frozen soil of $W^{30}T^{10}$ and $W^{30}T^{20}$ samples were thawed completely after 12 h, but $W^{30}T^5$ only thawed about 1/4 volume. Although we did not have direct evidence of the soil porosity changes under different thawing temperatures, it is not inconceivable that the air, free water, and ice crystals coexist in semithawed soil (**Figure 6**). We speculate that under moderate moisture and low thawing temperature, F–T cycles allowed for unique redox conditions favorable to N_2O production in nitrification and denitrification, and the semithawed state also provides large soil voids and ice openings for N_2O to move to the atmosphere.

In this study, the N_2O emissions of the W^{15} and W^{30} groups, respectively, peaked at the 3rd/4th cycles and 13th cycles, similar to previous studies (1st–9th cycles) (Teepe et al., 2001; Bollmann

and Conrad, 2004; Wu et al., 2019). Nutrient availability is widely regarded as the main reason for the massive release of N_2O during short F–T events (Risk et al., 2013; Congreves et al., 2018). This hypothesis holds that fragmented soil aggregates (Chai et al., 2014) and microbial mortality during F–T can release small molecular organic N (NH_4^+, NO_3^-, and amino acid) (Yanai et al., 2011; Yu et al., 2011). The abundant metabolic substrates stimulate microbial activities and accelerate N_2O production. Our previous study also demonstrated that the available N explained 30% of the variation in N_2O fluxes during spring thawing (Chen et al., 2018). Subsequent studies also confirmed that dissolved organic matter and inorganic N jointly regulate N_2O flux from soils with different moistures during a freeze–thaw period (Wu et al., 2019).

Accordingly, it is easy to understand the sharp increase in emissions during the 1st–13th F–T cycles of W^{15} and W^{30} treatments. However, previous studies showed that available N increased rapidly only in the first to fourth F–T cycles, and then, the contents stabilized after multiple repeated cycles (Grogan et al., 2004; Yu et al., 2011). This means that the promotion of N_2O emissions due to the increase in effective N over long-term F–T cycles is limited. However, the emission period of our study lasted until the 27th (W^{15}) and 48th (W^{30}) cycles. Moreover, the cumulative emissions of W^{15} and W^{45} were still increasing after 80 F–T cycles. Contrasting with the short-term effects of F–T on other seasonally frozen soil, frequent F–T disturbance may cause longer N transformation in alpine grasslands. Therefore, we suspected that the nutrient release in dry soil persisted during the long-term F–T cycles, and the N conversion pattern was different from that in soil with high moisture. The effect of F–T on the decomposition of soil organic matter in alpine grasslands under different water gradients needs further study.

The Model of N$_2$O Flux During Freeze–Thaw Cycles Under Global Change

This model (**Figure 6**) can provide some guidance for predicting the response of N_2O emissions in the nongrowing season under climate change, especially during spring thaw or snow melt. As our results showed, F–T disturbances drive N conversion and accelerate greenhouse gas (N_2O) emissions. Therefore, exploring the response of the soil C and N cycles to F–T events under different ecosystems of hydrothermal coupling is also necessary to predict the impacts and feedback of climate change in cold regions. Under the current climate, Wang et al. (2013) found that N_2O emissions of alpine meadow soil during spring thaw were 6.79 mg m^{-2}, accounting for 11% of emissions for the year. This *in situ* site is 30 km away from our sampling area. Although the value is much lower than our results, the warmer climate results in the topsoil undergoing many more F–T cycles and consequently prolongs the N_2O emission period in spring thawing and increases the proportion of emissions during the nongrowing season.

The current research shows that the climate of the QTP has become warmer and wetter, and the increased precipitation is mainly concentrated in the growing season

(Zhang Y. H. et al., 2016). This means that if the rainfall/snowfall increased in late September or early March, as our results suggested, this change would probably aggravate soil N_2O emissions in dry ecosystems, such as meadow and steppe. The large gaseous N loss may further reduce N availability and even limit N supply during the wet season. However, the annual total evapotranspiration (522.28 mm) of this region was larger than precipitation (447.30 mm), and in winter, almost all snowfall was returned to the atmosphere directly via evapotranspiration. Moreover, the temperature increase in winter ($0.45°C$ 10 a^{-1}) is nearly twice that in summer (Qin, 2014). Thus, topsoil would become drier in the nongrowing season. According to our prediction, dry soil would have reduced N_2O loss during F–T compared with wet soil. N_2O release from alpine grasslands may thus be a negative feedback to global warming. However, it cannot be ignored that the lower water levels of the alpine swamp in winter in the QTP possibly accelerated the succession of the swamp into a meadow or steppe ecosystem (Levy, 2008; Liu et al., 2018). This consequently exposed more peat soil and converted waterlogged soil to soil with a moderate moisture level.

It is estimated that the alpine meadow, steppe, and swamp in the QTP have approximately 133.52 Pg of organic C in the 0–0.75 m profile soils (Wang et al., 2002) and 16.08 Pg total N (Liu et al., 2012). Once the barrier of water and/or ice layer was lost in swamp soil, we detected that more than 1,000 times the normal level of N_2O would be released during F–T cycles. The large N pool size together with significant F–T cycles suggests a high risk of N_2O emissions and positive climate feedback across the alpine swamp. A past work has established that precipitation overrides warming in mediating soil N pools in an alpine grassland

ecosystem on the QTP (Lin et al., 2016), but these studies are based on the growing season, and the mechanisms of F–T cycles on the soil N pools when the soil moisture and temperature change simultaneously in alpine ecosystems are still not clear.

DATA AVAILABILITY STATEMENT

The original contributions presented in the study are included in the article/supplementary material, further inquiries can be directed to the corresponding authors.

AUTHOR CONTRIBUTIONS

ZC, WW, and HZ: conception and design of study. PL and YZ: acquisition of data. SG, ZZ, YD, BY, and HX: analysis and/or interpretation of data. All authors contributed to the article and approved the submitted version.

FUNDING

REFERENCES

Bollmann, A., and Conrad, R. (2004). Influence of O_2 availability on NO and N_2O release by nitrification and denitrification in soils. *Glob. Chang. Biol.* 4, 387–396. doi: 10.1046/j.1365-2486.1998.00161.x

Bracho, R., Natali, S., Pegoraro, E., Crummer, K. G., Schädel, C., Celis, G., et al. (2016). Temperature sensitivity of organic matter decomposition of permafrost-region soils during laboratory incubations. *Soil Biol. Biochem.* 97, 1–14. doi: 10.1016/j.soilbio.2016.02.008

Brooks, P. D., Grogan, P., Templer, P. H., Groffman, P., Öquist, M. G., and Schimel, J. (2011). Carbon and nitrogen cycling in snow-covered environments. *Geogr. Compass* 5, 682–699. doi: 10.1111/j.1749-8198.2011.00420.x

Chai, Y. J., Zeng, X. B., Bai, L. Y., Su, S., and Huang, T. (2014). Effects of freeze-thaw on aggregate stability and the organic carbon and nitrogen enrichment ratios in aggregate fractions. *Soil Use Manag.* 30, 507–516. doi: 10.1111/sum.12153

Chen, L., Liang, J., Qin, S., Liu, L., Fang, K., Xu, Y., et al. (2016). Determinants of carbon release from the active layer and permafrost deposits on the Tibetan Plateau. *Nat. Commun.* 7:13046.

Chen, Z., Yang, S. Q., Zhang, A. P., Jing, X., Song, W. M., Mi, Z. R., et al. (2018). Nitrous oxide emissions following seasonal freeze-thaw events from arable soils in northeast China. *J. Integr. Agric.* 17, 231–246. doi: 10.1016/s2095-3119(17)61738-6

Chen, Z., Yang, S. Q., Zhang, Q. W., Zhou, H., Jing, X., Zhang, A., et al. (2016). Effects of freeze-thaw cycles on soil nitrogen loss and availability. *Acta Ecol. Sin.* 36, 1083–1094.

Congreves, K. A., Wagner-Riddle, C., Si, B. C., and Clough, T. (2018). Nitrous oxide emissions and biogeochemical responses to soil freezing-thawing and drying-wetting. *Soil Biol. Biochem.* 117, 5–15. doi: 10.1016/j.soilbio.2017.10.040

Dai, L. C., Guo, X. W., Zhang, F. W., Du, Y., Ke, X., Li, Y., et al. (2019). Seasonal dynamics and controls of deep soil water infiltration in the seasonally-frozen

region of the Qinghai-Tibet plateau. *J. Hydrol.* 571, 740–748. doi: 10.1016/j.jhydrol.2019.02.021

Elberling, B., Michelsen, A., Schädel, C., Schuur, E. A. G., Christiansen, H. H., Berg, L., et al. (2013). Long-term CO2 production following permafrost thaw. *Nat. Clim. Chang.* 3, 890–894. doi: 10.1038/nclimate1955

Fang, X. W., Luo, S. Q., Lyu, S. H., Chen, B., Zhang, Y., Ma, D., et al. (2016). A simulation and validation of CLM during freeze-thaw on the Tibetan Plateau. *Adv. Meteorol.* 2016:9476098. doi: 10.1155/2016/9476098

Gaëlle, S., Christoph, M., Jean-Pierre, D., and Rebetez, M. (2011). Seasonal trends and temperature dependence of the snowfall/precipitation-day ratio in Switzerland. *Geophys. Res. Lett.* 38, 128–136.

Grogan, P., Michelsen, A., Ambus, P., and Jonasson, S. (2004). Freeze-thaw regime effects on carbon and nitrogen dynamics in sub-arctic heath tundra mesocosms. *Soil Biol. Biochem.* 36, 641–654. doi: 10.1016/j.soilbio.2003.12.007

Henry, H. A. L. (2008). Climate change and soil freezing dynamics: historical trends and projected changes. *Clim. Change* 87, 421–434. doi: 10.1007/s10584-007-9322-8

IPCC (2013). *Climate Change: The Physical Science Basis. Contribution of Working Group I to the Fifth Assessment Report of the Intergovernmental Panel on Climate Change.* Cambridge: Cambridge University Press, 1535. doi: 10.1017/CBO9781107415324

Ji, Q., Babbin, A. R., Jayakumar, A., Oleynik, S., and Ward, B. B. (2015). Nitrous oxide production by nitrification and denitrification in the Eastern Tropical South Pacific oxygen minimum zone. *Geophys. Res. Lett.* 42, 755–764.

Jiang, N., Juan, Y., Tian, L., Chen, X., Sun, W., and Chen, L. (2020). Soil water contents control the responses of dissolved nitrogen pools and bacterial communities to freeze-thaw in temperate soils. *Biomed. Res. Int.* 2020:6867081. doi: 10.1155/2020/6867081

Kreyling, J., Peršoh, D., Werner, S., Benzenberg, M., and Wöllecke, J. (2012). Short-term impacts of soil freeze-thaw cycles on roots and root-associated fungi

of *Holcus lanatus* and *Calluna vulgaris*. *Plant Soil* 353, 19–31. doi: 10.1007/s11104-011-0970-0

Kuang, X., and Jiao, J. (2016). Review on climate change on the Tibetan Plateau during the last half century. *J. Geophys. Res. Atmos.* 121, 3979–4007. doi: 10.1002/2015jd024728

Lawrence, D. M., Slater, A. G., and Swenson, S. C. (2012). Simulation of present-day and future permafrost and seasonally frozen ground conditions in CCSM4. *J. Clim.* 25, 2207–2225. doi: 10.1175/jcli-d-11-00334.1

Levy, J. K. (2008). Spatiotemporal vegetation cover variations in the Qinghai-Tibet Plateau under global climate change. *Chin. Sci. Bull.* 53, 915–922. doi: 10.1007/s11434-008-0115-x

Li, J. B., Zhao, Y., Zhang, A. F., Song, B., and Hill, R. L. (2021). Effect of grazing exclusion on nitrous oxide emissions during freeze-thaw cycles in a typical steppe of Inner Mongolia. *Agric. Ecosyst. Environ.* 307:107217. doi: 10.1016/j.agee.2020.107217

Li, Y. N., Zhao, X. Q., Cao, G. M., Zhao, L., and Q-X, Wang (2004). Analyses on climates and vegetation productivity background at Haibei Alpine meadow ecosystem research station. *Plateau Meteorol.* 23, 558–567.

Lin, L., Wang, Q. B., Zhang, Z. H., and He, J. S. (2017). Warming enhances soil freezing and thawing circles in the non-growing season in a Tibetan Alpine Grassland. *Acta Sci. Nat. Univ. Pekinensis* 53, 171–178.

Lin, L., Zhu, B., Chen, C. R., Zhang, Z., Wang, Q. B., and He, J. S. (2016). Precipitation overrides warming in mediating soil nitrogen pools in an alpine grassland ecosystem on the Tibetan Plateau. *Sci. Rep.* 6:31438.

Liu, H. Y., Mi, Z. R., Lin, L., Wang, Y., Zhang, Z., Zhang, F., et al. (2018). Shifting plant species composition in response to climate change stabilizes grassland primary production. *Proc. Natl. Acad. Sci. U.S.A.* 115, 4051–4056. doi: 10.1073/pnas.1700299114

Liu, W. J., Chen, S. Y., Qin, X., Baumann, F., Scholten, T., Zhou, Z., et al. (2012). Storage, patterns, and control of soil organic carbon and nitrogen in the northeastern margin of the Qinghai–Tibetan Plateau. *Environ. Res. Lett.* 7:035401. doi: 10.1088/1748-9326/7/3/035401

Lu, Z. D., Du, R., and Du, P. R. (2015b). Influences of land use/cover types on nitrous oxide emissions during freeze-thaw periods from waterlogged soils in Inner Mongolia. *PLoS One* 10:e0139316. doi: 10.1371/journal.pone.0139316

Lu, Z. D., Du, R., Du, P. R., Li, Z., Liang, Z., Wang, Y., et al. (2015a). Effect of mowing on N2O and CH4 fluxes emissions from the meadow-steppe grasslands of Inner Mongolia. *Front. Earth Sci.* 9:473–486. doi: 10.1007/s11707-014-0486-z

Ludwig, B., Wolf, I., and Teepe, R. (2004). Contribution of nitrification and denitrification to the emission of N2O in a freeze-thaw event in an agricultural soil. *J. Plant Nutr. Soil Sci.* 167, 678–684. doi: 10.1002/jpln.200421462

Lv, W., Luo, C., Zhang, L., Niu, H., Zhang, Z., Wang, S., et al. (2020). Net neutral carbon responses to warming and grazing in alpine grassland ecosystems. *Agric. For. Meteorol.* 280:107792. doi: 10.1016/j.agrformet.2019.107792

Mao, C., Kou, D., Chen, L. Y., Qin, S., Zhang, D., Peng, Y., et al. (2020). Permafrost nitrogen status and its determinants on the Tibetan Plateau. *Glob. Chang. Biol.* 26, 5290–5302. doi: 10.1111/gcb.15205

Mao, C., Kou, D., Wang, G., Peng, Y., Yang, G., Liu, F., et al. (2019). Trajectory of topsoil nitrogen transformations along a thermo erosion gully on the Tibetan Plateau. *J. Geophys. Res. Biogeosci.* 124, 1342–1354. doi: 10.1029/2018JG004805

Öquist, M. G., Nilsson, M., Sörensson, F., Kasimir-Klemedtsson, A., Persson, T., Weslien, P., et al. (2004). Nitrous oxide production in a forest soil at low temperatures-processes and environmental controls. *FEMS Microbiol. Ecol.* 49, 371–378. doi: 10.1016/j.femsec.2004.04.006

Qin, D. H. (2014). *Ecological Protection and Sustainable Development of Three-River Source Region*. Beijing: Science Press, 29–30.

Risk, N., Snider, D., and Wagner-Riddle, C. (2013). Mechanisms leading to enhanced soil nitrous oxide fluxes induced by freeze-thaw cycles. *Can. J. Soil Sci.* 93, 401–414. doi: 10.4141/cjss2012-071

Schuur, E. A. G., Mcguire, A. D., Schädel, C., Grosse, G., Harden, J. W., Hayes, D. J., et al. (2015). Climate change and the permafrost carbon feedback. *Nature* 520, 171–179.

Song, W. M., Wang, H., Wang, G. S., Chen, L., Jin, Z., Zhuang, Q., et al. (2015). Methane emissions from an alpine wetland on the Tibetan Plateau: neglected but vital contribution of the nongrowing season. *J. Geophys. Res. Biogeosci.* 120, 1450–1490.

Teepe, R., Brumme, R., and Beese, F. (2001). Nitrous oxide emissions from soil during freezing and thawing periods. *Soil Biol. Biochem.* 33, 1269–1275. doi: 10.1016/s0038-0717(01)00084-0

Teepe, R., Vor, A., Beese, F., and Ludwig, B. (2004). Emissions of N2O from soils during cycles of freezing and thawing and the effects of soil water, texture and duration of freezing. *J. Urmia Nurs. Midwifery Fac.* 63, 24–27.

Wang, G. S., Yang, X. X., Ren, F., Zhang, Z., and He, J. S. (2013). Non-growth season's greenhouse gases emission and its yearly contribution from alpine meadow on Tibetan Plateau of China. *Chin. J. Ecol.* 32, 1994–2001.

Wang, G. X., Qian, J., Cheng, G. D., and Yuanmin, L. (2002). Soil organic carbon pool of grassland soils on the Qinghai-Tibetan Plateau and its global implication. *Sci. Total Environ.* 291, 207–217. doi: 10.1016/s0048-9697(01)01100-7

Wang, Q. L., Wang, X., Cao, G. M., Wang, C. T., and Long, R. J. (2011). Soil quality assessment of alpine meadow in Haibei State of Qinghai Province. *Chin. J. Appl. Ecol.* 22, 1416–1422.

Wang, Y., Liu, H., Chung, H., Yu, L., Mi, Z., Geng, Y., et al. (2014). Non-growing-season soil respiration is controlled by freezing and thawing processes in the summer monsoon-dominated Tibetan alpine grassland. *Glob. Biogeochem. Cycles* 28, 9–20.

Wipf, S., Sommerkorn, M., Stutter, M. I., Wubs, E. R. J., and van der Wal, R. (2015). Snow cover, freeze-thaw, and the retention of nutrients in an oceanic mountain ecosystem. *Ecosphere* 6, 1–16.

Wu, H., Xingkai, X., Cheng, W., and Lin, H. (2019). Dissolved organic matter and inorganic N jointly regulate greenhouse gases fluxes from forest soils with different moistures during a freeze-thaw period. *Soil Sci. Plant Nutr.* 66, 163–176. doi: 10.1080/00380768.2019.1667212

Wu, X., Chen, Z., Kiese, R., Fu, J., Gschwendter, S., Schloter, M., et al. (2020). Dinitrogen (N2) pulse emissions during freeze-thaw cycles from montane grassland soil. *Biol. Fertil. Soils* 56, 959–972. doi: 10.1007/s00374-020-01476-7

Xu, W., Zhu, M. Y., Zhang, Z. H., Ma, Z., Liu, H., Chen, L., et al. (2017). Experimentally simulating warmer and wetter climate additively improves rangeland quality on the Tibetan Plateau. *J. Appl. Ecol.* 55, 1486–1497. doi: 10.1111/1365-2664.13066

Yanai, Y., Toyota, K., and Okazaki, M. (2007). Response of denitrifying communities to successive soil freeze-thaw cycles. *Biol. Fertil. Soils* 44, 113–119. doi: 10.1007/s00374-007-0185-y

Yanai, Y., Toyota, K., and Okazaki, M. (2011). Effects of successive soil freeze-thaw cycles on soil microbial biomass and organic matter decomposition potential of soils. *Soil Sci. Plant Nutr.* 50, 821–829. doi: 10.1080/00380768.2004.10408542

Yang, G., Peng, Y., Marushchak, M. E., Chen, Y., Wang, G., Li, F., et al. (2018). Magnitude and pathways of increased nitrous oxide emissions from uplands following permafrost thaw. *Environ. Technol.* 52, 9162–9169. doi: 10.1021/acs.est.8b02271

Yao, Z. S., Wu, X., Wolf, B., Dannenmann, M., Butterbach-Bahl, K., Brüggemann, N., et al. (2010). Soil-atmosphere exchange potential of NO and N₂O in different land use types of Inner Mongolia as affected by soil temperature, soil moisture, freeze-thaw, and drying-wetting events. *J. Geophys. Res. Atmos.* 115:D17116.

Yu, X. F., Zou, Y. C., Jiang, M., Lu, X., and Wang, G. (2011). Response of soil constituents to freeze-thaw cycles in wetland soil solution. *Soil Biol. Biochem.* 43, 1308–1320. doi: 10.1016/j.soilbio.2011.03.002

Zhang, K. P., Shi, Y., Jing, X., He, J. S., Sun, R., Yang, Y., et al. (2016). Effects of short-term warming and altered precipitation on soil microbial communities in Alpine Grassland of the Tibetan Plateau. *Front. Microbiol.* 7:1032. doi: 10.3389/fmicb.2016.01032

Zhang, Y. H., Cao, T., Kan, X., Wang, J., and Tian, W. (2016). Spatial and temporal variation analysis of snow cover using MODIS over Qinghai-Tibetan Plateau during 2003-2014. *J. Indian Soc. Rem. Sens.* 45, 1–11.